Linear and Regular Star Polymer in a Good Solvent

Giuseppe Allegra,* Emanuele Colombo, and Fabio Ganazzoli

Dipartimento di Chimica, Politecnico di Milano, via Mancinelli 7, I-20131 Milano, Italy

Received May 5, 1992; Revised Manuscript Received October 15, 1992

ABSTRACT: The conformational expansion problem of a regular star polymer in a good solvent is solved within the Gaussian approximation for the interatomic distances. Taking the Rouse-Zimm-Kilb Fourier coordinates as the basis of the conformational representation, their strain ratios with respect to the unperturbed phantom state are derived via self-consistent minimization of the intramolecular free energy. As usual for polymers above the Θ temperature, only the two-atom repulsions are taken into consideration. In the crossover regime, for an overall mean-square expansion up to 3, the off-diagonal strain ratios are less than $^1/_{10}$ the diagonal terms for a six-arm star and at least 1 order of magnitude smaller for a linear chain, thus indicating that the Fourier coordinates approach the normal modes to within a good approximation. Numerical analysis of the off-diagonal strain ratios is consistent with the expansion being especially large in the vicinity of the branch point, where the intramolecular repulsion is most concentrated. The mean-square expansion of the radius of gyration increases with $\tau N^{1/2}$ ($\tau = (T - \Theta)/T$, N is the number of atoms in the molecule) in about the same way as in the linear molecule. Bond correlation is largest around the branch point for bond vectors belonging to the same arm, but it tends to vanish if the bonds are on different arms. The normalized Kratky plot of the structure factor vs $Q = 4\pi \sin(\vartheta/2)/\lambda$ increases with increasing expansion at larger Q, consistent with a decrease of the normalized density $\rho(R)/\rho(0)$ for distances R from the center of mass on the order of the root-mean-square radius of gyration $\langle S^2\rangle^{1/2}$. The relative fluctuation of $\langle S^2\rangle$, that is, $(\langle S^4\rangle - \langle S^2\rangle^2)/\langle S^2\rangle^2$, is also shown to increase with increasing expansion. The present conformational study may be considered as a preliminary step to obtain the dynamic eigenfunctions as well as the relaxation times.

1. Introduction

There is a rising interest in the thermodynamic study of star polymers,[1-13] originated by the new potential insight on the intramolecular forces and conformations of different polymer architectures, obtainable today by increasingly sophisticated synthetic techniques.[3,6,14] Within a program aimed at the systematic theoretical investigation of regular star chains in dilute solution at different temperatures above or below the Θ point,[15] here we report an equilibrium conformational study of regular star polymers in a good solvent ($T > \Theta$). An additional scope of this work is that it provides the necessary information to obtain the dynamic eigenfunctions and the spectrum of relaxation times.[16]

We follow the self-consistent approach based on the Gaussian approximation for the probability distribution of the interatomic distances.[16] Confining our attention to the large molecular weight limit, we use a coarse-grained model where a finite number of evenly spaced representative beads are the points of concentration of the intramolecular forces. For convenience, the terms "atoms" and "bonds" will still be used to designate the beads and their connecting links. The intramolecular potential will be identified with the sum of all the interatomic long-range repulsions proportional to $\tau \cdot \langle r^2\rangle^{-3/2}$, where $\langle r^2\rangle$ is the mean-square distance between the two atoms and $\tau = (T - \Theta)/T$ is the reduced temperature. In a truly stereochemical approach based on the Gaussian approximation, the sum of the interatomic contributions should be carried out starting from a lower cutoff $\bar{k}$, equal to a few tens of bonds separating any two atoms.[15] In the spirit of the present coarse-grained model, in the following we shall put $\bar{k} = 1$ throughout. The two-body screened interactions $\propto \langle r^2\rangle^{-5/2}$, arising from shorter-range excluded volume repulsions not compensated by solvent-induced attractions even at $T = \Theta$, will be neglected in our large-chain limit as they can be absorbed in a suitable expansion of the interatomic bond.[15,16] The three-body and higher-order interactions will also be neglected, following a common procedure; as shown elsewhere, they are nicely absorbable in the two-body potential, after a suitable downward shift of the Θ temperature.[15,17,18] Only for star polymers with a large number (possibly $\gtrsim 10$) of short branches, n-body repulsions ($n \geq 3$) involving atoms from three or more different branches may play a significant role, possibly leading to stretching-out of the arms, as pointed out by Daoud and Cotton[12] and by Birshtein and Zhulina.[13] Overall, the relative weight of these multibranch repulsions is also bound to vanish in the infinite molecular weight limit.

After a section dealing with the Fourier basis set of the star polymer normal modes, the self-consistent optimization of the free energy will be discussed. In a subsequent section giving the numerical results for a star with six branches and different values of the reduced temperature, it will be shown that the Fourier modes deviate appreciably from orthogonality, although not very seriously, as a result of the peculiar concentration of interatomic repulsions in the core of the star; the cross terms may be estimated within the present scheme. The equilibrium structure factor will then be evaluated, and its connection with the atomic density around the center of mass will be discussed.

2. Normal Coordinates of the Regular Star Polymer

The total number of atoms is $N + 1$ and N/f their number within each of the f equal branches, all of them connected to a central atom. We associate a vector $\mathbf{l}^{(r)}(h)$ to each bond, oriented toward an increasing contour distance from the branch point; h ranges from 1 to N/f, moving from the branch point to the free end of the rth branch (see Figure 1). Let us consider the $N \times N$ correlation matrix $\mathbf{M}$, whose general element is the average scalar product of two bond vectors:

$$M_{(r-1)N/f+h,(s-1)N/f+j} = \langle \mathbf{l}^{(r)}(h) \cdot \mathbf{l}^{(s)}(j) \rangle \qquad (1)$$

Since $\mathbf{M}$ is real and symmetric, the normal coordinates, i.e., the statistically orthogonal vector combinations $\tilde{\mathbf{L}}(1)$, ..., $\tilde{\mathbf{L}}(N)$, may be derived from a unitary matrix $\mathbf{V}$ diagonalizing $\mathbf{M}$. We have

0024-9297/93/2226-0330$04.00/0

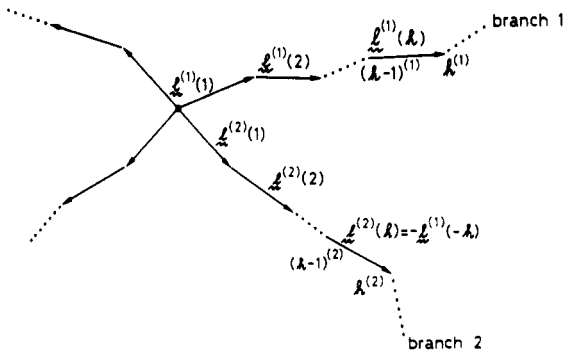

Figure 1. Scheme of the indexing of atoms and bonds for a star polymer.

$$\mathbf{V}^{*T}\cdot\mathbf{M}\cdot\mathbf{V} = \mathbf{\Lambda}\ \text{(diagonal)} \qquad \mathbf{V}\cdot\mathbf{V}^{*T} = \mathbf{E} \tag{2}$$

$$[\tilde{\mathbf{L}}(1)\tilde{\mathbf{L}}(2)...\tilde{\mathbf{L}}(N)] = [\mathbf{l}^{(1)}(1)\mathbf{l}^{(1)}(2)...\mathbf{l}^{(f)}(N/f)]\cdot\mathbf{V}$$

Given the equivalence of all the star branches, the structure of $\mathbf{M}$ is

$$\mathbf{M} = \begin{bmatrix} \mathbf{M}_0 & \mathbf{M}_1 & \mathbf{M}_1 & ... & \mathbf{M}_1 \\ \mathbf{M}_1 & \mathbf{M}_0 & \mathbf{M}_1 & ... & \mathbf{M}_1 \\ ... & & & & \\ \mathbf{M}_1 & \mathbf{M}_1 & \mathbf{M}_1 & ... & \mathbf{M}_0 \end{bmatrix} \tag{3}$$

where the $(N/f) \times (N/f)$ submatrices $\mathbf{M}_0$ and $\mathbf{M}_1$ are defined as

$$M_{0,hj} = \langle \mathbf{l}^{(r)}(h)\cdot\mathbf{l}^{(r)}(j)\rangle$$

$$M_{1,hj} = \langle \mathbf{l}^{(r)}(h)\cdot\mathbf{l}^{(s)}(j)\rangle \qquad r \neq s$$

$$\langle [\mathbf{l}^{(r)}(h)]^2\rangle = l^2 \tag{4}$$

Otherwise said, $\mathbf{M}_0$ and $\mathbf{M}_1$ comprise average products between bond vectors *on the same branch* and *on different branches*, respectively. $\mathbf{M}$ may be reduced to block-diagonal form $\mathbf{\Lambda}_{\text{block}}$ with the similarity transformation

$$\mathbf{\Lambda}_{\text{block}} = \mathbf{X}^*\cdot\mathbf{M}\cdot\mathbf{X} = \begin{bmatrix} \mathbf{M}_0 + (f-1)\,\mathbf{M}_1 & \mathbf{0} & \mathbf{0} & ... & \mathbf{0} \\ \mathbf{0} & \mathbf{M}_0 - \mathbf{M}_1 & \mathbf{0} & ... & \mathbf{0} \\ \mathbf{0} & \mathbf{0} & \mathbf{M}_0 - \mathbf{M}_1 & ... & \mathbf{0} \\ ... & & & & \\ \mathbf{0} & \mathbf{0} & \mathbf{0} & ... & \mathbf{M}_0 - \mathbf{M}_1 \end{bmatrix} \tag{5}$$

$$\mathbf{X} = f^{-1/2}\begin{bmatrix} \mathbf{E} & \mathbf{E} & ... & \mathbf{E} \\ \mathbf{E} & \mathbf{E}e^{i\varphi} & ... & \mathbf{E}e^{i(f-1)\varphi} \\ \mathbf{E} & \mathbf{E}e^{2i\varphi} & ... & \mathbf{E}e^{2i(f-1)\varphi} \\ ... & & & \\ \mathbf{E} & \mathbf{E}e^{i(f-1)\varphi} & ... & \mathbf{E}e^{i(f-1)^2\varphi} \end{bmatrix} \qquad \varphi = 2\pi/f \tag{5'}$$

where $\mathbf{E}$ is the unit matrix of order N/f. We see that eigenvalues and eigenvectors may be collected in two classes, the first one with a unit multiplicity deriving from $\mathbf{M}_0 + (f-1)\mathbf{M}_1$, the second one with multiplicity $(f-1)$ deriving from $\mathbf{M}_0 - \mathbf{M}_1$.

The normal-coordinate problem consists of diagonalizing these two matrices under the appropriate boundary conditions. Let us first remark that in the important, although special, case of the freely-jointed phantom chain both $(\mathbf{M}_0 + (f-1)\mathbf{M}_1)$ and $(\mathbf{M}_0 - \mathbf{M}_1)$ are diagonal in themselves, since $\langle \mathbf{l}^{(r)}(h)\cdot\mathbf{l}^{(s)}(j)\rangle = l^2\delta_{hj}\delta_{rs}$. As a result, *any* rotation matrix would perform the diagonalization, and the normal coordinates might be chosen with a wide freedom. The resulting degeneracy is removed whenever bond correlation exists. As an example, in the linear phantom chain with local stereochemical interactions, apart from usually negligible end effects, the matrix $\mathbf{M}$ is cyclic and its elements $\langle \mathbf{l}(h)\cdot\mathbf{l}(j)\rangle$ vanish quickly with an increasing difference $|j-h|$. Diagonalization of $\mathbf{M}$ is thus basically reduced to the same problem as diagonalization of the Rouse matrix $\mathbf{A}$ in the dynamics of the free-draining, freely-jointed linear chain; the eigenfunctions are given by linear bond vector combinations with Fourier coefficients that vanish exactly after the end bonds, in keeping with the boundary conditions.[19] Besides, as previously shown by Zimm and Kilb,[20] the star has specific symmetry requirements. Good-solvent expansion may affect the inner parts more strongly than the free ends, with the consequence that the resulting conformational inhomogeneity may cause the Fourier-type Rouse–Zimm–Kilb bond vector combinations to depart from the exact normal coordinates or eigenfunctions. In the following, we shall assume these vector combinations as our basis set (see Appendix), searching for their mean-square amplitudes as well as for the mean values of their cross-products (i.e., the off-diagonal elements). The Gaussian approximation for all of the interatomic distances will be adopted, and the self-consistent free energy optimization will be carried out. After the full correlation matrix of the Fourier components is obtained, the conformational problem is solved. Equations A-2–A-4 of the Appendix show that our basis-set coordinates are the vector elements[21] of $\tilde{\mathbf{L}}_{\text{anti}}$ and of $\tilde{\mathbf{L}}_{\text{sym}}$, with the respective multiplicities of 1 and $(f-1)$. Their correlation matrix is

$$\gamma = \begin{bmatrix} \alpha & & & & \\ & \beta & & & \\ & & \beta & & \\ & & & ... & \\ & & & & \beta \end{bmatrix} = l^{-2}\langle \tilde{\mathbf{L}}^T\cdot\tilde{\mathbf{L}}\rangle = l^{-2}\mathbf{V}^{*T}\cdot\mathbf{M}\cdot\mathbf{V}$$

$$\tilde{\mathbf{L}} = [\underbrace{\tilde{\mathbf{L}}_{\text{anti}}\ \ \tilde{\mathbf{L}}_{\text{sym}}\ \ \tilde{\mathbf{L}}_{\text{sym}}\ \ ...}_{(f-1)\text{ times}}] \tag{6}$$

where the basis-set vector $\tilde{\mathbf{L}}$ is given by

$$\tilde{\mathbf{L}} = \mathbf{L}\cdot\mathbf{V}$$

$$\mathbf{L} = [\mathbf{l}^{(1)}(1)\mathbf{l}^{(1)}(2)...\mathbf{l}^{(1)}(N/f)\mathbf{l}^{(2)}(1)...\mathbf{l}^{(2)}(N/f)...\mathbf{l}^{(f)}(1)\ ...\ \mathbf{l}^{(f)}(N/f)] \tag{7}$$

$$\mathbf{V} = \mathbf{X}\cdot\begin{bmatrix} \mathbf{A} & & & & \\ & \mathbf{B} & & & \\ & & \mathbf{B} & & \\ & & & ... & \\ & & & & \mathbf{B} \end{bmatrix} \qquad \mathbf{V}\cdot\mathbf{V}^{*T} = \mathbf{E} \tag{8}$$

and the matrices $\mathbf{A}$ and $\mathbf{B}$ are defined in eqs A-4.

In the case of short-range bond interaction establishing uniform correlation between bonds, so that their average scalar product only depends on their topological separation, γ is a diagonal matrix and $\tilde{\mathbf{L}}$ is the set of the normal coordinates. In the good-solvent regime at $T > \Theta$ both of the assumptions of uniformity and short-range bond correlation are generally unwarranted. Consequently, the Fourier coordinates are not generally an orthogonal set; i.e., α and β are not diagonal.

Although in principle α and β may be rendered diagonal, thus obtaining the normal coordinates in general, this is not necessary in the equilibrium case, as it will be shown in the following. In fact, the self-consistent optimization

process enables us to evaluate all of the elements of α and β, in principle, wherefrom all of the relevant equilibrium averages may be obtained. Since the diagonal elements of α and β indicate the amount of strain the mean-square Fourier amplitudes undergo with respect to the phantom state, henceforth for simplicity all of the elements of these matrices will be denoted as strain ratios.

3. Free Energy Self-Consistent Optimization

a. Mean-Square Distances. We shall distinguish between interatomic distances within the same branch and across different branches. In the former case, labeling with h and j the two atoms ($0 \le h < j \le N/f$, 0 being the branch point and N/f the free end) and labeling as 1 the branch comprising the two atoms, we have

$$\langle r^2(h,j)\rangle_{11} = \langle [\sum_{k=h+1}^{j} \mathbf{l}^{(1)}(k)]^2\rangle = \mathbf{P}_{hj}^T \cdot \mathbf{M} \cdot \mathbf{P}_{hj} \qquad (9)$$

where $\mathbf{M}$ is defined in eq 1 and the vector $\mathbf{P}_{hj}^T$ is

$$\mathbf{P}_{hj}^T = [00...11...10...0] \qquad (10)$$

the sequence of 1's beginning at position $h+1$ and ending at position j. In case the two atoms lie on different branches, the first and the second atoms will be taken on branches 1 and 2, respectively, and we write ($0 \le h,j \le N/f$)

$$\langle r^2(h,j)\rangle_{12} = \langle [\sum_{k=1}^{h} \mathbf{l}^{(1)}(k) - \sum_{k'=1}^{j} \mathbf{l}^{(2)}(k')]^2\rangle \qquad (11)$$

considering that the vector $\mathbf{r}(h,j)$ is given by $\mathbf{r}(h,0) - \mathbf{r}(j,0)$. Proceeding in analogy with eq 9 we write

$$\langle r^2(h,j)\rangle_{12} = \mathbf{Q}_{hj}^T \cdot \mathbf{M} \cdot \mathbf{Q}_{hj} \qquad (12)$$

where

$$\mathbf{Q}_{hj}^T = \Big[1\,1\,..\,\overset{(h)}{1}\,0\,0\,..\,0\,\overset{(N/f+1)}{-1}\,-1\,..\,-1\,\overset{(N/f+j)}{-1}\,0\,..\,0\Big] \qquad (13)$$

the position of each element being given by the upper symbol in parentheses. Equations A-4 and A-5 of the Appendix enable us to express $\mathbf{M}$ as a function of the Fourier-transformed matrices α and β. From

$$\mathbf{M} = l^2 \mathbf{V} \cdot \gamma \cdot \mathbf{V}^{*T}$$

$$\gamma = \begin{bmatrix} \alpha & 0 & ... & 0 \\ 0 & \beta & ... & 0 \\ ... & & \beta & .. \\ & & & .. \end{bmatrix} \qquad (14)$$

using eqs 5′, A-4, and A-5 we get from eqs 9 and 12

$$\langle r^2(h,j)\rangle_{1t} = (l^2/f)\sum_{n,m=1}^{N/f} \{a_{hj}^{(n)} a_{hj}^{(m)} \alpha_{nm} + [(f-1) b_{hj}^{(n)} b_{hj}^{(m)} + 2f(1-\delta_{1t}) b_{0h}^{(n)} b_{0j}^{(m)}]\beta_{nm}\} \qquad (15)$$

where

$$a_{hj}^{(n)} = C \cdot \sin [q_{2n}(j+h)/2] \sin [q_{2n}(j-h)/2]/\sin (q_{2n}/2) \qquad (16)$$

$$b_{hj}^{(n)} = C \cdot \cos [q_{2n-1}(j+h)/2] \sin [q_{2n-1}(j-h)/2]/\sin (q_{2n-1}/2) \qquad (16')$$

$$q_j = \pi j/(2N/f+1) \qquad C = 2/(2N/f+1)^{1/2} \qquad (16'')$$

From the mean-square distances, we may also get the mean-square radius of gyration in terms of the normal modes

$$\langle S^2\rangle = [2(N+1)^2]^{-1} \sum\sum_{h,j} \langle r^2(h,j)\rangle$$

$$= l^2[4(N+1)]^{-1} \sum_{m=1}^{N/f} \left[\frac{\alpha_{mm}}{\sin^2 (q_{2m}/2)} \left(1 + \frac{2-f}{N+1}\right) + (f-1)\frac{\beta_{mm}}{\sin^2 (q_{2m-1}/2)} \right] + l^2 \frac{2-f}{4(N+1)^2} \sum_{n\neq m=1}^{N/f} \frac{\alpha_{nm}}{\sin\left(\frac{q_{2n}}{2}\right) \sin\left(\frac{q_{2m}}{2}\right)} \qquad (17)$$

since for the unperturbed phantom chain $\alpha_{nm} = \beta_{nm} = \delta_{nm}$, we get, in the limit $N \to \infty$

$$\langle S^2\rangle_0 = \frac{Nl^2}{6} \frac{3f-2}{f^2} \qquad (17')$$

b. Intramolecular Free Energy. The free energy of the isolated molecule is given by, in $k_B T$ units[15,16]

$$\mathcal{A} = \mathcal{A}_{el} + \mathcal{A}_{intra} \qquad (18)$$

where the elastic component $\mathcal{A}_{el}$ has a purely entropic origin, whereas $\mathcal{A}_{intra}$ is due to the intramolecular contacts. In the general case where α and β are not diagonal $\mathcal{A}_{el}$ is given by[15]

$$\mathcal{A}_{el} = (3/2)\{\mathrm{Tr}\,\alpha - N/f - \ln (\mathrm{Det}\,\alpha) + (f-1)[\mathrm{Tr}\,\beta - N/f - \ln (\mathrm{Det}\,\beta)]\}$$

$$= (3/2)\{\sum_{n=1}^{N/f} [\alpha_{nn} - 1 + (f-1)(\beta_{nn} - 1)] - \ln (\mathrm{Det}\,\alpha) - (f-1) \ln (\mathrm{Det}\,\beta)\} \qquad (19)$$

a result that derives from the following equation, valid for truly orthogonal coordinates

$$\mathcal{A}_{el} = (3/2)\sum_{n=1}^{N/f} \{[\alpha_{nn} - 1 - \ln \alpha_{nn}] + (f-1)[\beta_{nn} - 1 - \ln \beta_{nn}]\} \qquad (19')$$

considering that neither the trace nor the determinant of a matrix changes after a similarity transformation. According to what was said in the Introduction, $\mathcal{A}_{intra}$ is simply given by a sum of the two-body long-range interactions, namely

$$\mathcal{A}_{intra} = \sum\sum_{h<j} a_2(h,j) \qquad (20)$$

$$a_2(h,j) = \tau B l^3 \langle r^2(h,j)\rangle^{-3/2} \qquad (20')$$

$$\tau = (T-\Theta)/T \qquad (20'')$$

and B is an appropriate adimensional parameter proportional to the effective volume per chain atom. In the above equations, the double sum is carried over all the ordered pairs of atoms h and j.

c. Self-Consistent Equations. The equilibrium conformation is determined by minimization of the overall free energy, given by eqs 18–20 together with eq 15, with respect to the strain ratios α_{nm} and β_{nm}. To simplify the

Table I
Polymers in a Good Solvent, $N/f = 200$

(i) Off-Diagonal Elements

	$\tau BN^{1/2}$	α_{12}	α_{13}	α_{23}	β_{12}	β_{13}	β_{23}	α_S^2
star, $f = 6$	0.35	−0.02	0.00	−0.01	−0.07	+0.03	−0.03	1.38
	1.39	−0.02	0.00	0.00	−0.18	+0.11	−0.08	2.11
	2.77	+0.01	−0.01	+0.02	−0.26	+0.19	−0.11	2.81
linear polymer, $f = 2$	3.00	+0.01	−0.00	+0.01	−0.01	+0.00	+0.01	2.94

(ii) Diagonal Elements

		α_{11}	α_{22}	α_{33}	β_{11}	β_{22}	β_{33}	α_S^2
star, $f = 6$, $\tau BN^{1/2} = 2.77$	full proced	2.14	1.79	1.65	3.11	2.06	1.80	2.81
	diag approx	2.02	1.77	1.64	3.20	2.07	1.79	2.87
linear, $f = 2$, $\tau BN^{1/2} = 3.00$	full proced	2.77	2.31	2.08	3.31	2.49	2.18	2.94

procedure, we shall assume the nonorthogonality effect to be small enough that the only nonzero off-diagonal elements α_{nm} and β_{nm} belong to the 3 × 3 upper-left submatrices of α and β. As we shall see, this simplification is admissible since nonorthogonality turns out to be especially localized among the most collective modes, whereas we have previously shown that modes with large indices are indeed orthogonal (see Appendix A of ref 22). Free energy minimization is obtained by setting $\partial\mathcal{A}/\partial\alpha_{nm} = 0$ (antisymmetric modes) and $\partial\mathcal{A}/\partial\beta_{nm} = 0$ (symmetric modes). The indices n and m either may coincide ($n = m \leq N/f$, diagonal terms) or may be different if both n and m are ≤3 (off-diagonal terms). Let us indicate that D_A and D_B, respectively, the determinants of the upper-left 3 × 3 submatrices of α and β and with $\sigma_{anti}(n,m)$ and $\sigma_{sym}(n,m)$ the following expressions

$$\sigma_{anti}(n,m) = \sum_{h=0}^{N/f-1}\sum_{j=h+1}^{N/f}\langle r^2(h,j)\rangle_{11}^{-5/2}a_{hj}^{(n)}a_{hj}^{(m)} + \frac{f-1}{2}\sum_{h=1}^{N/f}\sum_{j=1}^{N/f}\langle r^2(h,j)\rangle_{12}^{-5/2}a_{hj}^{(n)}a_{hj}^{(m)} \quad (21)$$

$$\sigma_{sym}(n,m) = \sum_{h=0}^{N/f-1}\sum_{j=h+1}^{N/f}\langle r^2(h,j)\rangle_{11}^{-5/2}b_{hj}^{(n)}b_{hj}^{(m)} + \sum_{h=1}^{N/f}\sum_{j=1}^{N/f}\langle r^2(h,j)\rangle_{12}^{-5/2}\left[\frac{f-1}{2}b_{hj}^{(n)}b_{hj}^{(m)} + fb_{0h}^{(n)}b_{0j}^{(m)}\right] \quad (21')$$

where $a_{hj}^{(n)}$ and $b_{hj}^{(n)}$ are reported in eqs 16 and the sets of indices (n, m, n') or, if $n = m$, (m, n', n'') coincide with (1, 2, 3). We get the result

antisymmetric modes

$$(n = m > 3) \quad (1 - \alpha_{nn}^{-1}) - \tau Bl^5\sigma_{anti}(n,n) = 0$$

$$(n = m \leq 3) \quad [1 - (\alpha_{n'n'}\alpha_{n''n''} - \alpha^2_{n'n''})/D_A] - \tau Bl^5\sigma_{anti}(n,n) = 0 \quad (21'')$$

$$(n \neq m;\ n,m \leq 3) \quad -(\alpha_{nn'}\alpha_{mn'} - \alpha_{nm}\alpha_{n'n'})/D_A - \tau Bl^5\sigma_{anti}(n,m) = 0$$

symmetric modes

α_{nm}, D_A, and $\sigma_{anti}(n,m)$ are respectively replaced by

β_{nm}, D_B, and $\sigma_{sym}(n,m)$

4. Numerical Results and Discussion

The coupled eqs 15 and 21 were solved self-consistently through a numerical iterative procedure identical to that employed in similar cases.[22,23] In the present work, the number of cycles required to achieve numerical stability for all of the values of α_{nm} and β_{nm} increases substantially with the number of arms even at a fixed arm length, due to the increasingly large number of cooperative interactions to be optimized near the branch point.

We shall discuss in the following some representative results obtained for a star with $f = 6$ and values of the solvent strength parameter τB leading to figures of $\alpha_S^2 = \langle S^2\rangle/\langle S^2\rangle_0$ up to 3, therefore being in the crossover regime (here and in the following the zero subscript stands for the unperturbed phantom polymer with $\tau B = 0$). The number of atoms per arm was 200.[24] The values of the α_{nm} and β_{nm} strain ratios with $n,m \leq 3$ are reported in Table I for three different values of τB; for comparison, the results in the diagonal approximation are also reported. We note that the first off-diagonal terms of the symmetric modes (β_{nm} with $n,m = 1, 2, 3$, $n \neq m$) are about 1 order of magnitude smaller than the corresponding diagonal terms, whereas the antisymmetric terms α_{nm} are still smaller by 1 more order of magnitude. As also shown in Table I, with linear chains (i.e., $f = 2$) under comparable conditions of expansion, both the symmetric and the antisymmetric off-diagonal terms are 2–3 orders of magnitude smaller than the corresponding diagonal terms. The difference derives from the much larger heterogeneity of the star polymer wherein strong repulsions across the branch point region induce a larger local expansion, the more so the larger is f; as a result, chain uniformity is lost and the basis-set coordinates tend to depart from the normal coordinates. The symmetric modes of the star are especially affected by the branch-point expansion because they represent centrosymmetrical conformations unlike the antisymmetrical modes. This explains the much smaller values of the off-diagonal α_{nm} terms than of the β_{nm}'s with the same indices (see Table I). It is possible to prove that, in the presence of a nonuniform expansion with a maximum in the star center, the sign of β_{nm} is given by $(-1)^{n+m}$, again in agreement with Table I. We remark that the diagonal strain ratios β_{nn} appear to be larger than α_{nn} if placed on an ideal smoothly decreasing function of q (where q is q_{2n} for α_{nn}, q_{2n-1} for β_{nn}; see eq A-4).

In the whole, the diagonal approximation appears to be reasonably good: in this case, the overall expansion ratio α_S^2 is only larger by no more than 2% than in the off-diagonal approach. Considering that the diagonal approximation effectively amounts to suppressing some degrees of freedom, this result indicates that *a larger expansion* is required if *a smaller number of degrees of freedom* are taken into consideration. The difference between the results with the off-diagonal strain ratios and those obtained in the diagonal approximation becomes

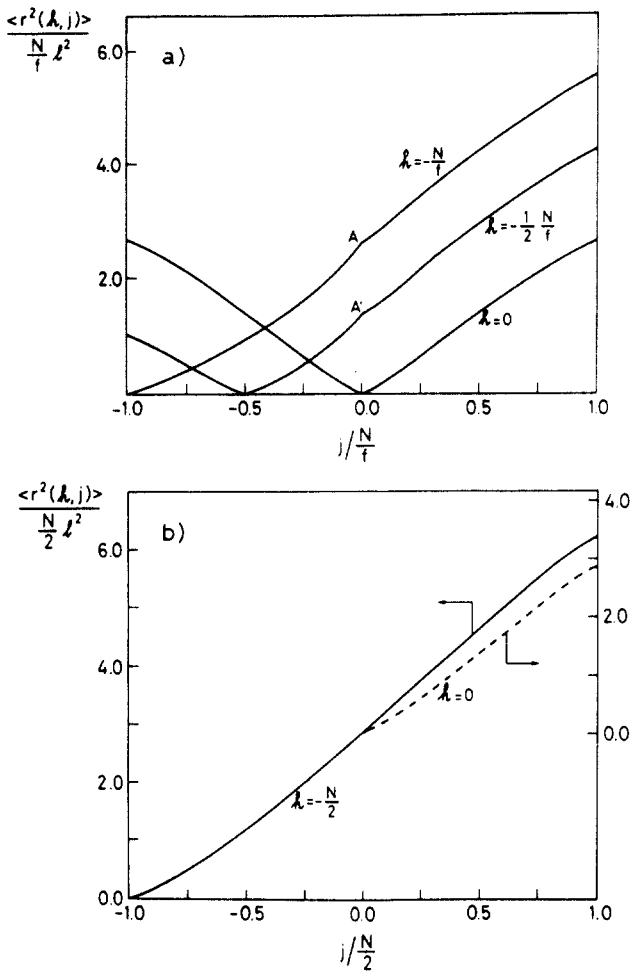

Figure 2. Reduced plots of $\langle r^2(h,j)\rangle$ for a star polymer (a, f = 6, α_S^2 = 2.81, results with off-diagonal elements) and for a linear chain (b, f = 2, α_S^2 = 2.94, results with off-diagonal elements). The atom indexes h and j are given as shown in Figure 1. For convenience, two branches of the same chain are considered, and the indexes are taken as negative ($-N/f$ through 0) on one and positive (0 through N/f) on the other. In (b) a vertical shift to the dashed line was applied, so that its origin coincides with the point giving $\langle r^2(-N/2,0)\rangle$.

vanishingly small if we consider the hydrodynamic radius (less than 0.1% with the largest τB), since this depends more heavily on the internal distances than does the mean-square radius of gyration. In fact, the internal short-range distances depend very little on the first modes, so that the effect of nonorthogonality is negligible. We conclude that the diagonal approximation is justified to a good degree of approximation; however, in the following we shall only refer to the results obtained with the inclusion of the off-diagonal terms.

The plot of the mean-square interatomic distances for the largest expansion degree (α_S^2 = 2.81) is shown in Figure 2a, where the bond labels run from $-N/f$ through 0 to $+N/f$ to encompass two different branches. Information on the intrachain vector correlation is easily derivable from the figure. Supposing $h < j$ for simplicity, regardless of the arm indices we may write

$$\langle r^2(h,j+1)\rangle = \langle[\mathbf{r}(h,j) + \mathbf{l}(j+1)]^2\rangle = \langle r^2(h,j)\rangle + l^2 + 2\langle \mathbf{r}(h,j)\cdot\mathbf{l}(j+1)\rangle \quad (22)$$

or, formally considering j as a continuous coordinate

$$\langle \mathbf{r}(h,j)\cdot\mathbf{l}(j+1)\rangle = {}^1/_2\frac{\partial\langle r^2(h,j)\rangle}{\partial j} - {}^1/_2 l^2 \quad (22')$$

Otherwise said, the slope of the plot of $\langle r^2(h,j)\rangle$ vs j at fixed h gives us the average correlation between $\mathbf{r}(h,j)$ and $\mathbf{l}(j+1)$.[25] Whereas this correlation is zero by definition in the random-walk chain, it may be shown to be always positive in the expanded state, approaching zero both for $j \to h$ and for $j \to N/f$, in agreement with Figure 2a. Besides, the sharp discontinuity in the slope of $\langle r^2(h,j)\rangle$ at j = 0 (see points A and A′ in Figure 2a) implies that the (end of branch)-to-(branch point) vector is strongly correlated with the bond adjoining the branch point on the *same* branch, whereas it is virtually uncorrelated with any other such bond on a *different* branch. In fact, if the atoms h and j belong to different uncorrelated branches, we should have $\langle r^2(h,j)\rangle_{12} \cong \langle r^2(h,0)\rangle_{11} + \langle r^2(j,0)\rangle_{11}$, where the branch point is labeled 0. This is seen indeed in Figure 2b, where we construct the sum $\langle r^2(h,0)\rangle_{11} + \langle r^2(j,0)\rangle_{11}$ using the linear chain (see the dashed curve), thus reproducing a plot similar to that in Figure 2a, $h = -N/f$. The physical reason of this loss of correlation across the branch point is rather simple: the repulsive interactions per se require increasing interatomic distances, thus increasing the average angle between any two branches. However, this inevitably implies decreasing the angles between all others. As a best compromise, the correlation *within* any arm is large and positive (see eq 22′), although it is lost across the branch point. Computer simulations would represent an ideal test for this prediction. The very accurate Monte Carlo simulations by Batoulis and Kremer[11] do indeed report bond vector correlation as a function of the topological separation. Unfortunately, they always chose to keep one of the bonds as the bond connected to the branch point, so that only the correlation *within* one arm was obtained.

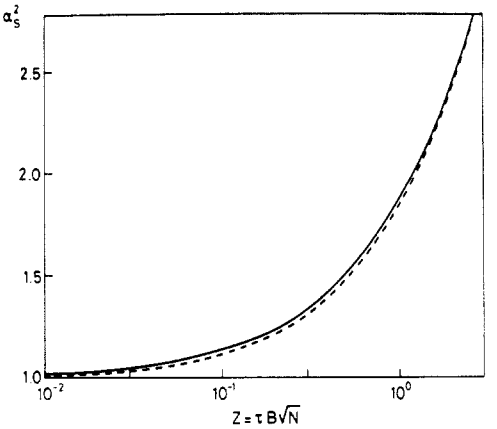

Figure 3. Logarithmic plot of $\alpha_S^2 = \langle S^2\rangle/\langle S^2\rangle_0$ vs $\tau BN^{1/2}$ (see text) for both the star polymer (solid line) and the linear chain (dashed line). (Results are from the calculation with off-diagonal elements.)

A plot of the expansion ratio $\alpha_S^2 = \langle S^2\rangle/\langle S^2\rangle_0$ as a function of $z = \tau BN^{1/2}$ is reported in Figure 3 for f = 6 in comparison with the linear chain (f = 2). The two curves differ very little, the ratio $\alpha_{S,\text{star}}^2/\alpha_{S,\text{lin}}^2$ at fixed z staying essentially constant and being only marginally larger than unity. We stress that for a given polymer type (i.e., a given B) and a given undercooling $\tau = (T-\Theta)/T$, the same variable z also implies the same N, that is, the same molecular weight, whereas the arm length N/f decreases with increasing f. *It is therefore implicit in Figure 3 that the expansion of the star polymer is much larger than that of the linear polymer having the same length as each star arm.*

It is useful to discuss the topological index g, which may be taken as a measure of the star polymer degree of

compactness; g is defined as

$$g = \langle S^2 \rangle_{star} / \langle S^2 \rangle_{lin} \tag{23}$$

the star and the linear polymer having the same molecular weight and the same τB. With reference to the unperturbed state, which may be identified with the phantom chain, or random-walk state in our assumption of very large molecular weights, we may write

$$g = g_0 \cdot \alpha^2_{S,star} / \alpha^2_{S,lin} \tag{24}$$

where[26]

$$g_0 = \langle S^2 \rangle_{0,star} / \langle S^2 \rangle_{0,lin} = (3f - 2)/f^2 \tag{25}$$

From the previous discussion on the expansion ratio α_S^2 we have the remarkable result that g is very close to, and only slightly larger than, g_0. Of course, this is simply due to the fact that the expansion of the star is very close to that of the linear chain, neither polymer being close to unperturbed. This somewhat fortuitous cancellation of effects was already pointed out by Douglas et al.[9] through renormalization group arguments. We should also note that in the perturbative approach, one has, to the first order in $z = \tau B N^{1/2}$ [27]

$$\alpha_S^2 = 1 + K_f z \tag{26}$$

the K_f coefficient depending only on f. It turns out that K_f increases rather slowly with f (in fact, $K_f \propto f^{1/2}$ for $f \to \infty$), so that we have, to the same order

$$g = g_{ph}[1 + (K_f - K_2)z] \tag{27}$$

with $K_2 = 134/105 = 1.276$ for the linear chain ($f = 2$). As an example, $K_6 = 1.449$, whence ($z \ll 1$)

$$g = 0.444 \cdot (1 + 0.173z) \tag{28}$$

According to our calculations, at larger z the term in parentheses tends to a constant value slightly larger than unity.

The above results are in essential agreement with experiment. Light scattering data suggest that indeed g is very close to g_0 for f up to 12[1] and possibly 18.[7-9] Using the zero and the Θ suffix to designate, respectively, the unperturbed state of the infinitely large polymer and of finite polymers, this result somehow conflicts with what is found in the Θ state, especially for short-branched stars with many arms. In fact, many experimental results[1,2,4,7] indicate $g_\Theta > g_0$ for $f > 8$, possibly as an effect of the n-body interactions ($n \geq 3$) which are particularly important for heavily branched stars; in a good solvent the three-body interactions may be neglected, so that we have $g_0 \lesssim g < g_\Theta$. However, some experimental data[1,4] suggest that this may not be completely true when f is quite large ($f \geq 18$) and/or the star arms are not long enough. Further problems may be due to an incomplete chemical synthesis reaction, so that in practice the expected number of arms is to be effectively regarded as an upper limit; obviously enough, the problem is more serious the larger is f. Similar results indicating $g \simeq g_0$ were also found in Monte Carlo simulations on a lattice.[10,11]

5. Structure Factor and Density Profile

The intensity profile of the scattered radiation, or structure factor, in the Gaussian approximation is given by

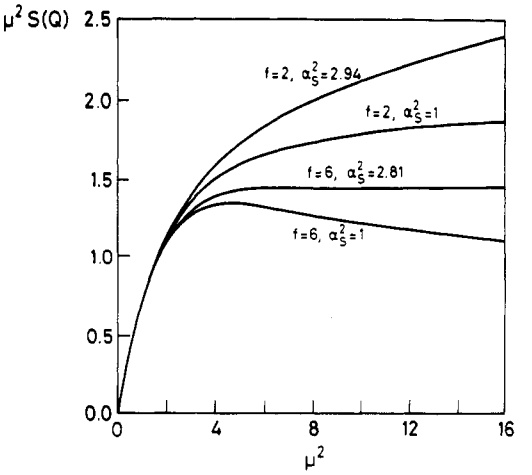

Figure 4. Kratky plot of $\mu^2 S(Q)$ vs μ^2 ($\mu^2 = Q^2\langle S^2 \rangle$, $Q = 4\pi \sin(\vartheta/2)/\lambda$) for the unperturbed and expanded star chain ($f = 6$, lower curves) and for the unperturbed and expanded linear chain ($f = 2$, upper curves). α_S^2 is the mean-square strain ratio of the radius of gyration.

$$S(Q) = (N+1)^{-2} \sum \sum_{h,j=0}^{N} \exp(-Q^2 \langle r^2(h,j) \rangle / 6) \tag{29}$$

where $Q = 4\pi \sin(\vartheta/2)/\lambda$; $S(Q)$ is normalized so that $S(Q = 0) = 1$. Figure 4 shows the normalized plots of $\mu^2 S(Q)$ vs μ^2, $\mu^2 = Q^2\langle S^2 \rangle$, for the star ($f = 6$) and the linear chain, each considered both in the unperturbed and in the most expanded state. We see that for both polymers the normalized scattering at large Q *increases* with increasing expansion. This result is strictly correlated with an increasing dispersion of the atoms around the center of mass, as it will be seen in the following. Labeling with $\langle R^2(h) \rangle$ the mean-square distance of the hth atom on any branch fron the center of mass, it may be shown that ($N \gg 1$)

$$\langle R^2(h) \rangle = (l^2/2N) \sum_{m=1}^{N/f} \left[\alpha_{mm} \frac{\cos^2(q_{2m}h)}{\sin^2(q_{2m}/2)} + (f-1)\beta_{mm} \frac{\sin^2(q_{2m-1}h)}{\sin^2(q_{2m-1}/2)} \right] \tag{30}$$

a result that in the ideal unperturbed case (i.e., $\alpha_{mm} \equiv \beta_{mm} = 1$) reduces to

$$\langle R^2(h) \rangle_0 = (Nl^2/3f^2) \left[1 + 3\frac{hf}{N}\left(\frac{hf}{N} + f - 2\right) \right] \tag{30'}$$

Since the probability of finding any atom at a distance R from the center of gravity is merely the sum of the separate probabilities for each atom, the isotropic probability density is

$$\rho(R) = f \sum_{h=1}^{N/f} \left(\frac{3}{2\pi \langle R^2(h) \rangle} \right)^{3/2} \exp\left(-\frac{3R^2}{2\langle R^2(h) \rangle} \right) + \left(\frac{3}{2\pi \langle R^2(0) \rangle} \right)^{3/2} \exp\left(-\frac{3R^2}{2\langle R^2(0) \rangle} \right) \tag{31}$$

the factor f being due to the statistical equivalence of all branches, whereas the last term is due to the branch point. Figure 5 shows the plots of $\rho(R)$ vs R for both the unperturbed and the expanded star ($\alpha_S^2 = 2.81$) with $f = 6$, obtained from eqs 30 and 31. We see that the ratio $\rho(R)/\rho(0)$ decreases upon expansion, the largest fractional

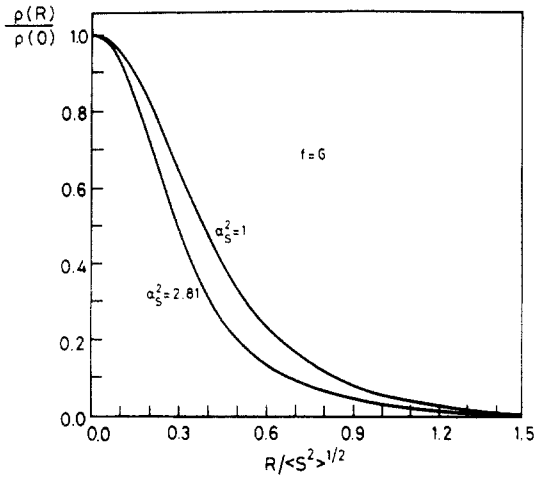

Figure 5. Reduced atomic density of the star chain ($f = 6$) vs $R/\langle S^2\rangle^{1/2}$, R being the distance from the polymer center of mass and $\langle S^2\rangle$ the mean-square radius of gyration. (Upper curve) Unperturbed state, $\alpha_S^2 = 1$, $\rho(0) = 1.196$ atoms/l^3. (Lower curve) Expanded state, $\alpha_S^2 = 2.81$, $\rho(0) = 0.395$ atoms/l^3.

decrease being at $\mathcal{R} = R/\langle S^2\rangle^{1/2}$ around unity. As a consequence, the ratio

$$(\langle S^4\rangle - \langle S^2\rangle^2)/\langle S^2\rangle^2 = \{\int_0^\infty \rho(R)4\pi R^6\,dR/[\int_0^\infty \rho(R)4\pi R^4 dR]^2\} - 1 \quad (32)$$

increases to 0.097, from the exact value 0.079 characteristic of the unperturbed state;[28] an analogous increase is also found with the linear chain, which shows that the fluctuations of $\langle S^2\rangle$ do increase compared to those of the unperturbed polymer. It should be added that any variation to the plot of $\rho(\mathcal{R})$ vs $\mathcal{R}$ induced by the solvent quality (i.e., expansion or contraction) must conform to the constraint

$$\int_0^\infty \rho(\mathcal{R})\mathcal{R}^2 d\mathcal{R} = \int_0^\infty \rho(\mathcal{R})\mathcal{R}^4 d\mathcal{R} \quad (33)$$

as it is easy to prove from the definition of $\langle S^2\rangle$ in terms of $\rho(R)$.

6. Concluding Remarks

The average solution-conformation properties of a regular star with any number f of branches are obtained through the self-consistent procedure of free energy minimization, within the Gaussian approximation for the interatomic distances.[16] We remark that, to the extent that the relaxation times are obtained from linearized equations of motion, the Gaussian approximation is the equilibrium counterpart. Solution of the equilibrium problem, as discussed in this paper, is therefore preliminary to the dynamic investigation. Attention being focused upon the good-solvent expansion regime at $T > \Theta$, only the two-body long-range repulsion terms are retained, whose free energy is proportional to $\langle r^2(h,j)\rangle^{-3/2}$, $r(h,j)$ being the distance between any two atoms. Shorter-range effects, such as the screened interactions $\propto \langle r^2(h,j)\rangle^{-5/2}$ due to residual hard-core repulsions, are absorbed in a suitably defined bond length l.[15,16] It is implied that the number of skeletal atoms is very large, although the calculations are carried out on a coarse-grained model consisting of a relatively small number of beads per branch (=200) connected by ideal springs (for simplicity, beads and connecting springs are respectively denoted atoms and bonds). The normal-mode analysis is carried out by using the Fourier bond vector combinations with pure sine or cosine coefficients, as the basis of the orthonormal eigenfunctions; in the assumption that these do not deviate very much from the pure Fourier modes, a relatively simple procedure to obtain the off-diagonal coefficients is suggested. Numerical calculations for six-arm stars in the crossover regime of good-solvent expansion show that the assumption is indeed valid in most usual cases, the off-diagonal averages of the pure Fourier modes never exceeding 10% of the largest diagonal average even at a mean-square expansion of about three over the unperturbed state, coinciding with the random-walk star in our coarse-grained model. Qualitative analysis of the off-diagonal values (see Table I) shows that they arise from a nonuniform expansion of the star, which is largest in the region around the branch point due to the highest concentration of interatomic repulsions. Obviously enough, for this very reason the relative weight of the off-diagonal terms is bound to increase with increasing f. Comparison with the diagonal-approximation results shows that the overall mean-square expansion is reduced by no more than 2% in the complete approach; however, this makes the overall strain to be more evenly distributed among the modes.

Analysis of the resulting interatomic distances (see Figure 2 and eq 22) shows that the strongest vector correlation takes place between the first bond attached to the branch point and the end-to-end vector of the same branch, thus suggesting that the overall space orientation of the branch is implicit in that of the first bond or of the few first bonds, on average. Conversely, bond correlation is strongly reduced *across* the branch point, so that the different branches are essentially uncorrelated one with another, the more so the larger is the number of branches. Also, bond correlation vanishes toward the free ends; i.e., the terminal bonds are uncorrelated with all the other bonds, as it may also be seen from the second equation given in footnote 25. As another result of this interplay of correlations, Figure 2 shows that, writing $\langle r^2(h,j)\rangle \propto |j - h|^{2\nu}$ to a rough approximation and considering it as a function of j for a fixed h, 2ν is *larger* than one (as expected) if h is made to coincide with a free end ($h = -N/f$), at least if j is not close to the other free end (i.e., if $j \approx N/f$); conversely, 2ν is (mostly) *smaller* than one if h coincides with the branch point ($h = 0$). Although insufficient experimental information is now available, small-angle neutron or X-ray experiments on properly chosen stars, perhaps after suitable chemical tagging, may provide a check for these predictions.

Figure 3 shows that the squared strain ratio of the radius of gyration $\alpha_S^2 = \langle S^2\rangle/\langle S^2\rangle_0$ of the regular star with $f = 6$ is only 2% at most larger than that of the linear chain with the same $\tau BN^{1/2}$ (τB is the expansion parameter per chain atom and N is their number). Since from the usual g ratio, defined as

$$g = \langle S^2\rangle_{star}/\langle S^2\rangle_{lin} \quad (34)$$

we have

$$\alpha_{S,star}^2/\alpha_{S,lin}^2 = g/g_0 \quad (35)$$

where g_0 is the Θ-state value for $N \to \infty$, we also get the result $g \simeq g_0$, in agreement with experimental data in good solvent (i.e., at large $\tau BN^{1/2}$) and with renormalization group results.[9] We note that the n-body repulsions ($n \geq 3$) among atoms placed on three or more different branches may become relevant for highly branched stars ($f > 10$) of low molecular weight. In this case, the approximation that polymer expansion is dominated by the two-body repulsions may be unwarranted.

The Kratky plot of the structure factor is predicted to increase at large $Q = 4\pi \sin(\vartheta/2)/\lambda$ as an effect of the polymer expansion, consistent with the similar effect obtained for the linear chain (see Figure 4). In turn, this is related with the decrease of the reduced density $\rho(R)/\rho(0)$ at $R/\langle S^2\rangle^{1/2} \simeq 1$ upon expansion, R being the distance from the center of mass (see Figure 5), and with an increasing ratio $\langle S^4\rangle/\langle S^2\rangle^2$, therefore with an increase of fluctuations of $\langle S^2\rangle$.

Acknowledgment. This work was financially supported by Consiglio Nazionale delle Ricerche (CNR, Italy), Progetto Finalizzato Chimica Fine, and by the Italian Ministry of University and of Scientific and Technological Research (MURST, 40%).

Appendix

To account for the vanishing of the intramolecular force at the branch ends, the basis-set coordinates will be given by

$$\tilde{\mathbf{L}}(k) = \sum_{h=1}^{N/f}\sum_{r=1}^{f} W_{khr}\mathbf{l}^{(r)}(h) \qquad \text{(A-1)}$$

where

$$W_{khr} = \sum_{m=1}^{N/f} a_{kmr}\sin[q_{2m}(h-1/2)] + \sum_{m=1}^{N/f} b_{kmr}\cos[q_{2m-1}(h-1/2)] \qquad \text{(A-1')}$$

$$q_j = \pi j/(2N/f+1)$$

It may be checked that $W_{khr} = 0$ for $h = N/f + 1$, consistent with the absence of a chain bond after the (N/f)th site on any branch.

The basis-set coordinates $\tilde{\mathbf{L}}(k)$ must also conform to the molecule symmetry. Let us first remark that $\mathbf{M}_0 + (f-1)\mathbf{M}_1$ and $\mathbf{M}_0 - \mathbf{M}_1$ (see eq 5) may be written as the following average dyadic products:

$$\mathbf{M}_0 + (f-1)\mathbf{M}_1 = \langle \mathbf{L}_{anti}^T \cdot \mathbf{L}_{anti}\rangle$$

$$\mathbf{L}_{anti} = f^{-1/2}[(\mathbf{l}^{(1)}(1) + \mathbf{l}^{(2)}(1) + \ldots + \mathbf{l}^{(f)}(1)), (\mathbf{l}^{(1)}(2) + \mathbf{l}^{(2)}(2) + \ldots + \mathbf{l}^{(f)}(2)), \ldots (\mathbf{l}^{(1)}(N/f) + \ldots + \mathbf{l}^{(f)}(N/f))] \qquad \text{(A-2)}$$

$$\mathbf{M}_0 - \mathbf{M}_1 = \langle \mathbf{L}_{sym}^T \cdot \mathbf{L}_{sym}\rangle$$

$$\mathbf{L}_{sym} = 2^{-1/2}[(\mathbf{l}^{(r)}(1) - \mathbf{l}^{(s)}(1)), (\mathbf{l}^{(r)}(2) - \mathbf{l}^{(s)}(2)), \ldots, (\mathbf{l}^{(r)}(N/f) - \mathbf{l}^{(s)}(N/f))] \quad (r \neq s) \qquad \text{(A-2')}$$

If $\mathbf{A}$ and $\mathbf{B}$ are two rotation matrices respectively diagonalizing $\mathbf{M}_0 + (f-1)\mathbf{M}_1$ and $\mathbf{M}_0 - \mathbf{M}_1$, the basis-set vectors deriving from $\mathbf{L}_{anti}$ and $\mathbf{L}_{sym}$ turn out to be

$$\tilde{\mathbf{L}}_{anti} = \mathbf{L}_{anti}\cdot\mathbf{A};\ \tilde{\mathbf{L}}_{sym} = \mathbf{L}_{sym}\cdot\mathbf{B} \qquad \text{(A-3)}$$

where $\mathbf{A}$ and $\mathbf{B}$ must share the same symmetry as $\mathbf{L}_{anti}$ and $\mathbf{L}_{sym}$, respectively. Considering first $\mathbf{L}_{sym}$ for convenience, we see from eqs A-2' and Figure 1 that analytical continuation of the vector sequence within $\mathbf{L}_{sym}$ toward negative bond indices such as $-1, -2, \ldots$ leads to identifying $\mathbf{l}^{(r)}(-h)$ with $-\mathbf{l}^{(s)}(h)$ and $-\mathbf{l}^{(s)}(-h)$ with $+\mathbf{l}^{(r)}(h)$, which leaves the difference $\mathbf{l}^{(r)}(h) - \mathbf{l}^{(s)}(h)$ unchanged upon changing h into $-h$. Otherwise said, the vector sequence within $\mathbf{L}_{sym}$ is *symmetrical* with respect to sign inversion of h, so that the $\mathbf{B}$ matrix is formed by the the *cosine* terms of eq A-1. Using a similar argument, $\mathbf{L}_{anti}$ is *antisymmetrical* with respect to h, since analytical continuation of the vector sum $\mathbf{l}^{(1)}(h) + \mathbf{l}^{(2)}(h) + \ldots + \mathbf{l}^{(f)}(h)$ from h to $-h$ implies its sign reversal, and we conclude that the matrix $\mathbf{A}$ is built up with the antisymmetrical *sine* terms of eq A-1'.[21]

We make now the simplest choice, namely that each element of $\mathbf{A}$ and $\mathbf{B}$ comprises a single term of the Fourier sum (eq A-1'). Consequently, their general element is given by

$$A_{hm} = C\cdot\sin[(h - {}^1/_2)q_{2m}]$$

$$B_{hm} = C\cdot\cos[(h - {}^1/_2)q_{2m-1}]$$

$$q_p = \pi p/(2N/f+1);\ C = 2/(2N/f+1)^{1/2} \qquad \text{(A-4)}$$

It is possible to check that the vector elements of $\tilde{\mathbf{L}}_{anti}$ and $\tilde{\mathbf{L}}_{sym}$ (see eq A-3) are indeed orthogonal if the requirements of short-range bond correlation and of conformational uniformity are met; the latter requirement implies that the average product between any two bond vectors only depends on their topological separation. We shall define now

$$\alpha = l^{-2}\langle \tilde{\mathbf{L}}_{anti}^T\cdot\tilde{\mathbf{L}}_{anti}\rangle = l^{-2}\mathbf{A}^T\cdot[\mathbf{M}_0 + (f-1)\mathbf{M}_1]\cdot\mathbf{A}$$

$$\alpha(n,m) = \alpha_{nm}$$

$$\beta = l^{-2}\langle \tilde{\mathbf{L}}_{sym}^T\cdot\tilde{\mathbf{L}}_{sym}\rangle = l^{-2}\mathbf{B}^T\cdot(\mathbf{M}_0 - \mathbf{M}_1)\cdot\mathbf{B}$$

$$\beta(n,m) = \beta_{nm} \qquad (n,m = 1, 2, \ldots, N/f) \qquad \text{(A-5)}$$

in agreement with eqs 6 of the main text.

References and Notes

(1) Roovers, J.; Hadjichristidis, N.; Fetters, L. J. *Macromolecules* **1983**, *16*, 214.
(2) Bauer, B. J.; Hadjichristidis, N.; Fetters, L. J.; Roovers, J. E. L. *J. Am. Chem. Soc.* **1980**, *102*, 2410.
(3) Hadjichristidis, N.; Roovers, J. E. L. *J. Polym. Sci., Polym. Phys. Ed.* **1974**, *12*, 2521.
(4) Huber, K.; Burchard, W.; Fetters, L. J. *Macromolecules* **1984**, *17*, 541.
(5) Huber, K.; Burchard, W.; Bantle, S.; Fetters, L. J. *Polymer* **1987**, *28*, 1990.
(6) Toporowski, P. M.; Roovers, J. *J. Polym. Sci., Polym. Chem. Ed.* **1986**, *24*, 3009.
(7) Bauer, B. J.; Fetters, L. J.; Graessley, W. W.; Hadjichristidis, N.; Quack, G. F. *Macromolecules* **1989**, *22*, 2337.
(8) Roovers, J.; Martin, J. E. *J. Polym. Sci., Polym. Phys. Ed.* **1989**, *27*, 2513.
(9) Douglas, J. F.; Roovers, J.; Freed, K. F. *Macromolecules* **1990**, *23*, 4618.
(10) Barrett, A. J.; Tremain, D. L. *Macromolecules* **1987**, *20*, 1687.
(11) Batoulis, J.; Kremer, K. *Macromolecules* **1989**, *22*, 4277.
(12) Daoud, M.; Cotton, J. P. *J. Phys.* **1982**, *43*, 531.
(13) Birshtein, T. M.; Zhulina, E. B. *Polymer* **1984**, *25*, 1453.
(14) Roovers, J. E. L.; Bywater, S. *Macromolecules* **1974**, *7*, 443.
(15) Allegra, G.; Ganazzoli, F. *Prog. Polym. Sci.* **1991**, *16*, 463.
(16) Allegra, G.; Ganazzoli, F. *Adv. Chem. Phys.* **1989**, *75*, 265.
(17) Cherayil, B. J.; Douglas, J. F.; Freed, K. F. *J. Chem. Phys.* **1985**, *83*, 5293; **1987**, *87*, 3089.
(18) Ganazzoli, F.; Allegra, G. *Macromolecules* **1990**, *23*, 262.
(19) Rouse, P. E. *J. Chem. Phys.* **1953**, *21*, 1272. Zimm, B. H. *J. Chem. Phys.* **1956**, *24*, 269.
(20) Zimm, B. H.; Kilb, R. W. *J. Polym. Sci.* **1959**, *37*, 19.
(21) It should be noted when applied to the *atomic position vectors* (instead of the bond vectors), the linear combination yielding $\mathbf{L}_{anti}$ (see eq A-2) gives rise to a *symmetrical* combination and $\mathbf{L}_{sym}$ (see eq A-2') to an *antisymmetrical* one. As a consequence,

cosines and sines must be interchanged in the Fourier modes. This is relevant when dealing with star polymer dynamics.

(22) Allegra, G.; Ganazzoli, F. *J. Chem. Phys.* **1982**, *76*, 6354.
(23) Ganazzoli, F.; Allegra, G. *Polymer* **1988**, *29*, 651.

(24) We report here a few details of the numerical procedure. At each iteration cycle, each of the eqs 21″ was solved for α_{nm} (β_{nm}) as the only unknown, all the other $\alpha_{n'm'}$'s ($\beta_{n'm'}$'s) and the value of D_A (D_B) being kept at the value of the previous cycle. To dampen out numerical fluctuations of the results, we entered each new cycle with a value of α_{nm} (β_{nm}) equal to the average of the figures used in the previous two cycles plus that resulting from eqs 21″. The number of cycles required to have fluctuations not exceeding $\pm 10^{-4}$ over all the α's (β's) ranged from 20 to 30, going from the lowest to the highest value of $\tau BN^{1/2}$.

(25) Correlation between bond vectors is given by the general equation $\langle \mathbf{l}(h)\cdot\mathbf{l}(j)\rangle = -(1/2)\partial^2\langle r^2(h,j)\rangle/\partial h\partial j$, which is not easily suited for comparison with Figure 2 (G. Allegra, M. De Vitis, and F. Ganazzoli, unpublished data). In terms of the strain ratios it may be shown that

$$\langle \mathbf{l}(h)\cdot\mathbf{l}(j)\rangle = (2/N)\sum_n [\alpha_{nn}\sin(hq_{2n})\sin(jq_{2n}) + (\delta_{1f}-1)\beta_{nn}\cos(hq_{2n-1})\cos(jq_{2n-1})]$$

(26) Zimm, B. H.; Stockmayer, W. H. *J. Chem. Phys.* **1949**, *17*, 1301.
(27) Berry, G. C.; Orofino, T. A. *J. Chem. Phys.* **1964**, *40*, 1614.

(28) This ratio tends to zero with increasing f, as suggested by the unperturbed value $(4/15)[(15f-14)/(3f-2)^2]$. As a general result in terms of the normal-mode strain ratios α_{nm} and β_{nm}, we have ($N \to \infty$) (Allegra, unpublished result)

$$(\langle S^4\rangle - \langle S^2\rangle^2)/\langle S^2\rangle^2 = {}^2/_3\sum_n [\alpha_{nn}^2/n^4 + \beta_{nn}^2/(n-{}^1/_2)^4]/\{\sum_n [\alpha_{nn}/n^2 + \beta_{nn}/(n-{}^1/_2)^2]\}^2$$